Available online at www.sciencedirect.com
ScienceDirect
International Journal of Heat and Mass Transfer 50 (2007) 4713–4723
International Journal of HEAT and MASS TRANSFER
www.elsevier.com/locate/ijhmt

Correlating heat transfer and friction in helically-finned tubes using artificial neural networks

Gregory J. Zdaniuk *, Louay M. Chamra, D. Keith Walters

Department of Mechanical Engineering, Mississippi State University, 210 Carpenter Engineering Building, P.O. Box ME, Mississippi State, MS 39762-5925, USA

Received 19 November 2006; received in revised form 5 March 2007
Available online 12 June 2007

Abstract

An artificial neural network (ANN) approach was used to correlate experimentally determined Colburn *j*-factors and Fanning friction factors for flow of liquid water in straight tubes with internal helical fins. Experimental data came from eight enhanced tubes with helix angles between 25° and 48°, number of fin starts between 10 and 45, fin height-to-diameter ratios between 0.0199 and 0.0327, and Reynolds numbers ranging from 12,000 to 60,000. The performance of the neural networks was found to be superior compared to the corresponding power-law regressions. The ANNs were subsequently used to predict data of other researchers but the results were less accurate. The ANN training database was therefore expanded to include experimental data from two independent investigations. The ANNs trained with the combined database showed satisfactory results, and were superior to algebraic power-law correlations developed with the combined database.

Keywords: Friction; Heat transfer; Helically-finned tube; Artificial neural networks

1. Introduction

Industrial use of heat transfer enhancement has become widespread. The goal of heat transfer enhancement is to reduce the size and cost of heat exchanger equipment. Webb [1] gives an excellent overview of different enhancement mechanisms available in commercial tubes.

One contemporary enhancement geometry is the helical fin shown in Fig. 1, which is described by several geometric variables. Fig. 1 also provides a pictorial description of these variables, which include: the fin height (e), the fin pitch (p), the helix angle (α), number of starts (N_s), and included angle (β). The fin height is the distance measured from the internal wall of the tube to the top of the fin. The fin pitch is the distance between the centers of two fins measured in the axial direction. The helix angle is the angle the fin forms with the tube axis. The number of starts refers to how many fins one can count around the circumference of the tube. Finally, the angle at which the sides of the fin meet is called the included angle.

An extensive literature survey of research on helically-finned tubes is given in Zdaniuk and Chamra [2]. Despite a considerable amount of study, the characteristics of flow inside helically-finned tubes are still not very well understood because the physics governing the flow are very complex and experimental data are limited. The current approach to predicting pressure drop and heat transfer in helically-finned tubes is to use algebraic correlations based on least-squares regression. Regression techniques performed on experimental data require mathematical functional form assumptions, which limit their accuracy and generality. To address these limitations, techniques that can effectively overcome the complexity of the problem without *ad hoc* assumptions are needed. One of these techniques is the artificial neural network (ANN), inspired by the biological network of neurons in the brain.

* Corresponding author. Tel.: +1 662 325 3261; fax: +1 662 325 7223.
E-mail address: zdaniuk@me.msstate.edu (G.J. Zdaniuk).

0017-9310/$ - see front matter © 2007 Elsevier Ltd. All rights reserved.
doi:10.1016/j.ijheatmasstransfer.2007.03.043

Nomenclature

b	node bias	St	Stanton number
D	tube diameter (m)	t	average fin width (m)
e	fin height (m)	w	weight
f	Fanning friction factor	W	weight matrix
F	node function	x	node input/output
j	Colburn j-factor: $j = StPr^{2/3}$		
MSE	mean squared error: MSE $= \frac{\sum(\text{value from experiment} - \text{predicted value})^2}{\text{number of measurements}}$	*Greek symbols*	
		α	helix angle (°)
N_s	number of fin starts	α' and α''	corrugation shape angles (°)
Nu	Nusselt number	β	included angle (°)
p	axial fin pitch (m)		
Pr	Prandtl number	*Superscript*	
Re	Reynolds number	*	refers to normalized network inputs and outputs
S	number of nodes in a layer		

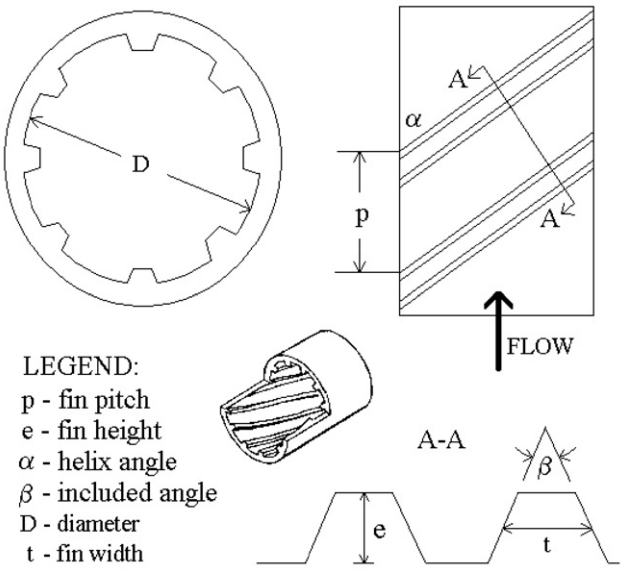

Fig. 1. A helically-finned tube and its geometry.

2. Artificial neural networks and heat transfer

Despite the complexity of the natural environment, living creatures are able to perform involved activities within their ecosystems. Animals can rapidly process vast amounts of data and make "calculated" decisions. This capability, attributed to the nervous system, is partly acquired and partly enhanced through a process called learning. Last century's advancements in bio-medical sciences have shed some light on the functioning of the nervous system. Studies in bio-medicine and psychology have attempted to understand the brain and its elementary component – the neuron. Knowledge gained in this topic encouraged scientists to apply the concept of a neuron to mathematics and logic, giving birth to artificial neural networks (ANNs).

The purpose of ANNs is to provide solution algorithms to complex problems such as classification, clustering, data compression, pattern association, function approximation, forecasting, control applications, or optimization. To many researchers dealing with these topics, ANNs are a subject of study in themselves. A brief introduction to the fundamentals of ANNs is given in Zdaniuk [3]. Readers who are interested in learning more about ANNs are encouraged to explore some of the many texts on this subject (e.g., Haykin [4] or Mehrotra et al. [5]).

Because ANNs have emerged relatively recently, their presence in the thermal science literature is limited. Section 3 describes several articles that describe how ANNs can be implemented successfully in heat transfer and fluid flow problems.

Thibault and Grandjean [6] were one of the early authors to show the use of ANNs in heat transfer data analysis. Thibault and Grandjean [6] solved three different heat transfer problems using three-layered, feed-forward ANNs: a thermocouple lookup table, a series of correlations between Nusselt and Rayleigh numbers for the free convection around horizontal smooth cylinders, and the problem of natural convection along slender vertical cylinders with variable surface heat flux. Thibault and Grandjean [6] concluded that neural networks can be used efficiently to model and correlate heat transfer data without the burden of finding appropriate model structures to fit experimental data. The disadvantage of ANNs is the impossibility, simply by inspection, of determining the influence that one variable has on an output variable. ANNs, therefore, lack the transparency of most standard mathematical expressions.

Sen and Yang [7] described the scope of ANNs and genetic algorithm techniques in thermal science applications including an exhaustive bibliography. Sen and Yang [7] presented two interesting examples that use ANNs to predict the performance of compact heat exchangers. The first heat exchanger was a single-row, fin-tube, cross-flow

air-to-water type, and the second one was similar but with more tube rows, air-side condensation, and variable fin spacing. The authors' purpose was to compare the mathematical correlations for heat transfer with an ANN approach. Sen and Yang [7] proved that in both cases the ANN approach yields more accurate results. The explanation is worth citing: "results suggest that the ANNs have the ability of recognizing all the consistent patterns in the training data including the relevant physics as well as random and biased measurement errors. (...) However, the ANN does not know and does not have to know what the physics is. It completely bypasses simplifying assumptions such as the use of coefficient of heat transfer. On the other hand, any unintended and biased errors in the training data set are also picked up by the ANN. The trained ANN, therefore, is not better than the training data, but not worse either." Finally, Sen and Yang [7] also demonstrated a successful application of ANNs for transient analysis of the first of the two heat exchangers.

Kalogirou [8] presented a review of various applications of ANNs in energy problems. The problems were classified into six thematic categories, and each category had subsections with specific examples as well as references. The categories described by Kalogirou [8] were as follows:

(1) Modeling various aspects of a solar steam generator.
(2) HVAC systems: estimation of building heating loads, prediction of energy use in commercial buildings, optimization of energy consumption by HVAC systems, or controlling a bus air conditioning system.
(3) Solar radiation.
(4) Modeling and control in power generation systems: combustion modeling, control of a thermal plant, or analysis of harmonic power distortion.
(5) Forecasting and prediction of power consumption and cost.
(6) Refrigeration: frost prediction on evaporator coils.

Ashforth-Frost et al. [9] described a multitude of uses of ANNs in heat transfer and fluid mechanics with emphasis on visualization processing techniques such as particle image velocimetry. The authors reported several references that used ANNs to recognize different geometric patterns in multiphase flows. In these cases, ANNs have replaced more manual methods. ANN modeling of physiological flows was also suggested as a solution to very complex medical analyses. Furthermore, the authors mentioned inverse problems as being good candidates for ANN treatment due to their sensitivity to noise and reported several successful examples reported in the literature.

ANNs were also used to correlate two-phase flow data. Kelleher et al. [10] investigated data from a series of experiments on R-114 and R-113 pool boiling heat transfer from a vertical bank of tubes with variable amounts of oil present in the refrigerant. Their objective was to employ the neural network technique as a method of using experimental data to predict heat transfer behavior and to make the heat transfer predictions more accurate than regular mathematical correlations, less reliant on assumptions, and easier to use. After training, Kelleher et al.'s [10] network was able to accurately predict the heat flux for 72 different tube correlations and varying superheat. The average percent errors were well under 10%.

Heat transfer literature is most abundant in examples of ANNs used for performance prediction and control of heat exchangers (as in [7]). A number of publications in this topic originated at the University of Notre Dame (Pacheco-Vega et al. [11–13], and Diaz et al. [14–17]). Another example worthy of note is Islamoglu [18] who used a feed-forward backpropagation ANN to predict heat transfer rates of a wire-on-tube type heat exchanger widely used in small refrigeration systems. Nineteen experiments were conducted in three air-flow modes: all cross-, wire cross-, and tube cross-flow. Islamoglu's [18] network had twelve input nodes (describing heat exchanger geometry and fluid flow rates), one output node corresponding to the heat flux, and one hidden layer with five nodes. The data were successfully correlated with a mean relative error of 4% (7.94% maximum relative error).

ANNs have also been used to characterize various flows inside tubes and channels. Ghajar et al. [19] used ANNs to significantly improve heat transfer correlations in the transition region for a circular tube with three different inlet configurations. Islamoglu and Kurt [20] trained an ANN to predict heat transfer from a channel with triangular corrugations. Scalabrin and Piazza [21] applied neural networks to analyze heat transfer from tubes with supercritical carbon dioxide. Chen et al. [22] analyzed spirally corrugated tubes in terms of ANNs. However, the focus was only on the shape of the corrugation and not the helix angle. Chen et al. [22] tested tubes with four starts, a similar pitch (~9 mm), diameter (~18.9 mm), ridge height (~2.2 mm), and helix angle (~61°) but different corrugation shapes. The shape of the corrugation was quantified in terms of angles α' and α'' as shown in Fig. 2. The authors devised a radial-basis function ANN that correlated the angles of the triangular groove, α' and α'', with the inside heat transfer coefficient. Next, they used the ANN to determine the optimal corrugation shape. The highest value for the heat transfer coefficient occurred at $\alpha'' \approx 90°$ and $\alpha' \approx 62°$. This result was outside of the range of tested tubes.

Albeit small, the number of publications described here indicates that ANNs can be used for a wide range of heat

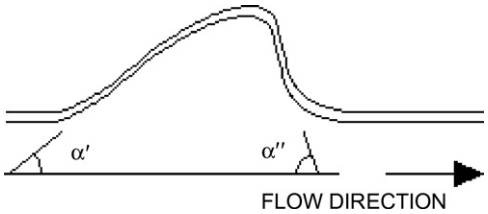

Fig. 2. Corrugation angles investigated by Chen et al. [22].

transfer and fluid problems. Nevertheless, ANNs have not been applied to correlate heat transfer and friction with all of the necessary geometric parameters of a helically-finned tube. Such attempt is made in this publication.

3. Experimental data

An experimental program devised to measure turbulent pressure drop and heat transfer in helically-finned tubes was conducted at Mississippi State University. The experimental apparatus and procedure are described in detail in Zdaniuk et al. [23]. Eight enhanced tubes and one plain tube were tested. The tubes were mounted horizontally in a straight annulus, forming a double-pipe counter-flow heat exchanger with hot water flowing on the tube side and cold water on the annulus side. The tubes were manufactured for condenser applications. The internal geometric parameters of each tube are delineated in Table 1. The tube material was copper-nickel. The internal fins were 0.48-mm thick at the base and 0.2-mm thick at the tip, yielding an included angle β of 41°. The dimensionless parameters e/D, p/e, and p/D were obtained by introducing the axial fin pitch, $p = \pi D/(N_s \tan\alpha)$ and calculating the dimensionless factors. These dimensionless parameters allow a more direct comparison between the tubes and provide more physical insight into the results. Table 1 does not explicitly indicate that the helix angle and the number of starts are dimensionless parameters. However, since these parameters are unitless, they can be treated as such. Therefore, α and N_s can be used as direct parameters in any correlation.

Experimentally determined Fanning friction factors and Colburn j-factors are plotted in Figs. 3 and 4. Zdaniuk et al. [23] calculated the uncertainty in the measured friction factor and heat transfer coefficient at 15% and 10%, respectively. Zdaniuk et al. [23] reported that the maximum percent difference between the plain tube measured friction factor and the value predicted by the Blasius equation was 11%. Furthermore, the maximum percent difference between the plain tube measured heat transfer coefficient and the value predicted by the Dittus–Boelter equation was 8%. Both errors being within the limits of experimental uncertainty validated the experimental apparatus.

Zdaniuk et al. [23] used a regression-based procedure to correlate the experimental data shown in Figs. 3 and 4 in the following manner:

Table 1
Internal geometry of the test tubes

Tube #	Internal structure					Dimensionless factors		
	D (mm)	e (mm)	p (mm)	N_s	α (°)	e/D	p/e	p/D
1	15.64	0.38	10.54	10	25	0.0243	27.729	0.674
2	15.61	0.375	3.51	30	25	0.0240	9.348	0.225
3	15.62	0.38	1.47	30	48	0.0243	3.876	0.0941
4	15.57	0.38	2.33	45	25	0.0244	6.134	0.150
5	15.6	0.31	1.56	45	35	0.0199	5.017	0.100
6	15.57	0.38	1.55	45	35	0.0244	4.085	0.100
7	15.59	0.51	1.55	45	35	0.0327	3.048	0.100
8	15.58	0.38	0.98	45	48	0.0244	2.577	0.0629
9	15.65	Plain						

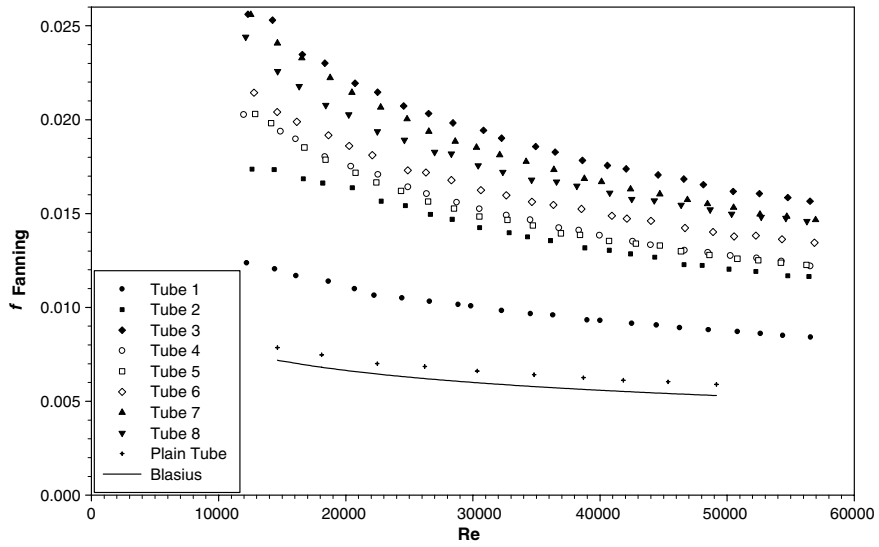

Fig. 3. Measured Fanning friction factors for the eight tube geometries used in the current study, plotted with the Blasius (smooth tube) correlation.

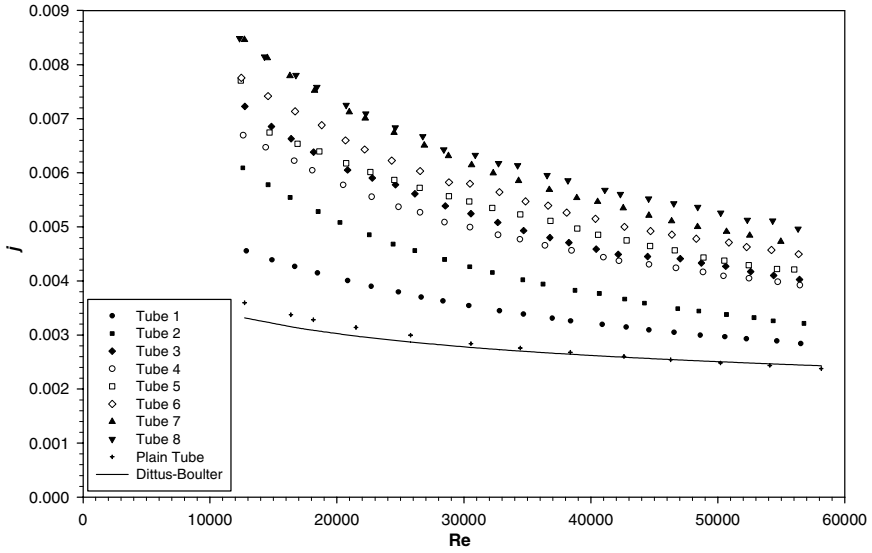

Fig. 4. Measured Colburn *j-factors* for the eight tube geometries used in the current study, plotted with the Dittus–Boelter (smooth tube) correlation.

$$f = 0.128Re^{-0.305}N_s^{0.235}(e/D)^{0.319}\alpha^{0.397} \quad (1)$$

$$j = 0.029Re^{-0.347}N_s^{0.253}(e/D)^{0.0877}\alpha^{0.362} \quad (2)$$

Eqs. (1) and (2) were shown to predict the vast majority of experimental data with an error of less than 10%. The mean squared prediction errors of Eqs. (1) and (2) were MSE = 1.070×10^{-6} and MSE = 6.945×10^{-8}, respectively.

4. Artificial neural network development

4.1. Notation

Fig. 5 shows a general three-layer ANN and the notation employed. Due to the large number of parameters involved, developing an unambiguous way of presenting the constants and functions that describe a neural network is important. In this study, the software employed for ANN development was MATLAB, so the notation presented here is almost identical to that used by MATLAB. The only difference is that MATLAB indexing must start at 1 and not 0; so in MATLAB, all the 0-indexed variables are essentially replaced by a different variable. The consistency of the notation presented herein allows MATLAB to execute computations at each layer rapidly because of its matrix algebra capability ([24]).

The index-0 layer represents inputs (see Fig. 5). $\boldsymbol{X}^0$ is a column vector of inputs of size S^0; whereas, S^1, S^2, and S^3 are the number of nodes in layer 1, 2, and 3, respectively. $\boldsymbol{W}^{1,0}$ is a weight matrix feeding the inputs to layer 1. The weight matrix is constructed such that entry $\boldsymbol{W}^{1,0}_{j,k}$ multiplies input k and feeds it into node j in layer 1. In general, $\boldsymbol{W}^{l,m}_{j,k}$ multiplies output k from layer m and feeds it into node j in layer l. $\boldsymbol{b}$ is the bias column vector. Its size corresponds to the number of nodes in a given layer. $\boldsymbol{F}$ is a vector of node functions (MATLAB feed-forward backpropagation networks utilize either linear, log-sigmoid, or tan-sigmoid functions) and generally, the same function is used for the entire layer.

The current study reports weights and biases as matrices and vectors, respectively, in the notation presented above. The names of the reported ANNs also contain the description of the network's architecture. For example, "f_ANN_4LS_3LS_1LIN" stands for a friction factor

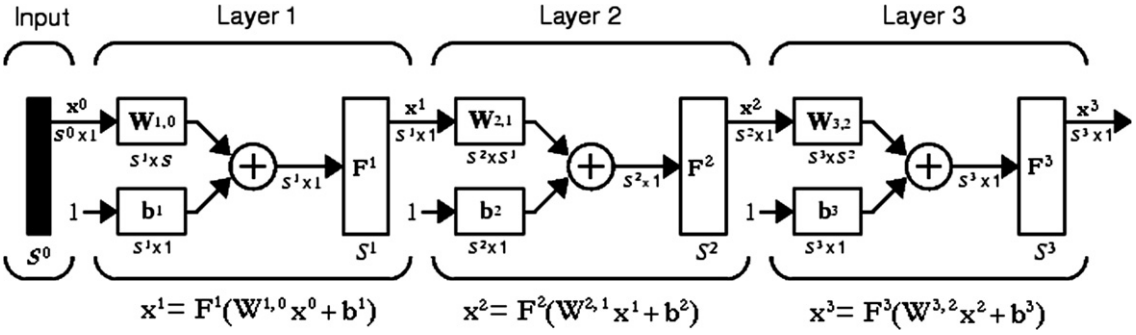

Fig. 5. Neural network notation.

network with 4 nodes in layer 1 using log-sigmoid functions [in MATLAB: $\text{logsig}(x) = 1/(1+\exp(-x))$], 3 nodes in layer 2 using log-sigmoid functions, and 1 node in layer 3 using a linear function [in MATLAB: *purelin*$(x) = x$].

4.2. Normalization of experimental data

When training ANNs, it is advantageous to normalize the inputs and targets to ensure that all the weights are within the same order of magnitude. The normalized data will be denoted with the symbol "*". The data from the current study have been normalized in the following fashion:

$$Re^* = \left(\frac{Re - 1800}{Re + 1800}\right)^2 \tag{3}$$

$$N_s^* = \frac{N_s}{100} \tag{4}$$

$$e/D^* = 10 \cdot e/D \tag{5}$$

$$\alpha^* = \sin(\alpha) \tag{6}$$

$$f^* = 10 \cdot f \tag{7}$$

$$j^* = 100 \cdot j \tag{8}$$

The significance of Eq. (3) is that it forces Re^* to zero if $Re = 1800$ (critical Reynolds number for transition) and to one if Re is large. The other normalizing equations have been chosen for their simplicity. Moreover, the inputs to every neural network in this study have been organized in the following manner:

$$x^0 = \begin{Bmatrix} N_s^* \\ \alpha^* \\ e/D^* \\ Re^* \end{Bmatrix} \tag{9}$$

4.3. Determination of optimal network architecture

The performance of an ANN depends on its architecture. Large networks can learn complex functions, but require more effort to train and to report. Hence, the network selection process is a compromise between a small network size and a minimal prediction error. The architecture of the optimal network to be used for prediction of friction and j-factors in helically-finned tubes was determined for this study by training different networks and evaluating their performance with the mean squared error (MSE) criterion. Half of the experimental data (every other Reynolds number) from each tube was put into a training basket, while the entire data set was used for validation. The Levenberg–Marquardt algorithm (Levenberg [25] and Marquardt [26]) was used for the training process. Training was stopped when the MSE of the entire data set reached a minimum. The training results were compiled in Table 2, which lists the MSEs of all networks trained with 50% of experimental data. The idea behind the selection of the various networks in Table 2 was to start out with an arbitrary 4-3-1 network and to remove nodes and layers to see what happens to the network's performance. Initially, one node was removed from each of the first two layers to yield a 3-2-1 network. Next, the second layer was removed to yield a 4-1 network. Then, a 2-1 network was constructed. For the 2-1 case, a log-sigmoid output node function was also tested, but showed no improvement in performance.

Table 2
Mean squared errors of ANNs trained with 50% of data

f		j	
Network	MSE	Network	MSE
f_4LS_3LS_1LIN	7.7760×10^{-9}	j_4LS_3LS_1LIN	1.0062×10^{-9}
f_3LS_2LS_1LIN	1.6848×10^{-8}	j_3LS_2LS_1LIN	2.2488×10^{-9}
F_4LS_1LIN	8.3616×10^{-9}	j_4LS_1LIN	1.9653×10^{-9}
F_2LS_1LIN	1.0061×10^{-7}	j_2LS_1LIN	6.3833×10^{-9}
F_2LS_1LS	1.1755×10^{-7}	j_2LS_1LS	6.5631×10^{-9}

Table 2 reveals that even the worst performing networks, f_2LS_1LS and j_2LS_1LS, have a smaller mean squared error than the power-law regression presented in Section 4.2 [Eqs. (1) and (2) showed, respectively, a MSE of 1.070×10^{-6} for f and a MSE of 6.945×10^{-8} for j]. The 4-3-1 architecture exhibited the smallest MSE. Removing one node from the first two layers deteriorated the networks' performance more than removing the second layer. Because of the large number of variables associated with the 4-3-1 networks, the 4-1 network appears to be the optimal architecture for prediction of f and j in helically-finned tubes. Additional information (i.e., weights, biases, and training curves) about the networks listed in Table 2 are given in Zdaniuk [3].

The use of the MSE is an excellent numerical criterion for evaluating the performance of a prediction tool. Nevertheless, a visual inspection of the error behavior is also very important. Consider the performance of the f_4LS_1LIN network depicted in Fig. 6 and the j_4LS_1LIN network

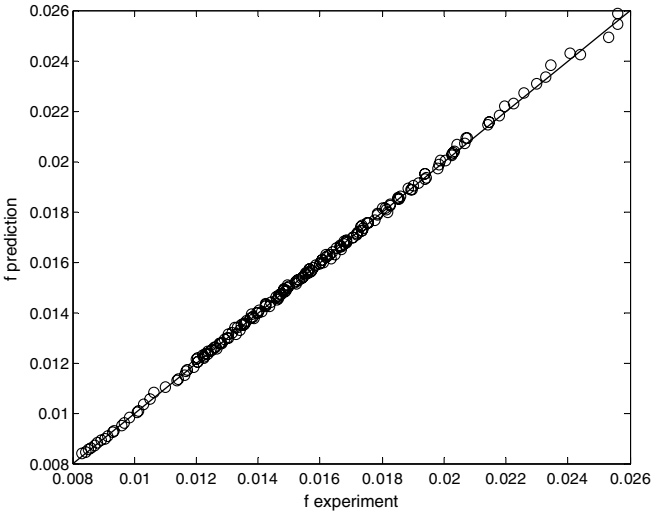

Fig. 6. Scatter plot indicating the performance of the f_4LS_1LIN ANN trained with 50% data.

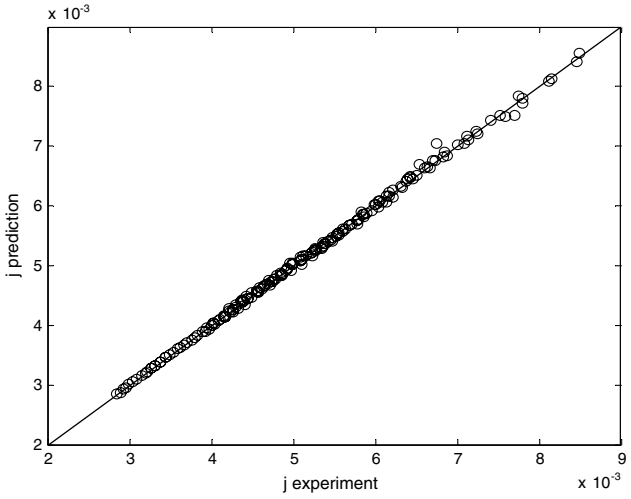

Fig. 7. Scatter plot indicating the performance of the j_4LS_1LIN ANN trained with 50% data.

in Fig. 7. Both networks were trained with 50% of experimental data as described earlier. Both figures clearly show that the 4-1 network geometry works very well. Based on this visual inspection and the MSE values of Table 2, the prediction (or "regression") error associated with the 4-1 ANNs trained with 50% of data can be taken as negligible compared to the experimental uncertainty.

The information presented so far demonstrates that the ANN does not know and does not have to know what the physics of the problem are. The ANN completely bypasses simplifying assumptions such as the use of a power-law equation. On the other hand, any unintended and biased errors in the training data set are also picked up by the ANN. As noted by Sen and Yang [7], the trained ANN is therefore not better than the training data, but not worse either.

4.4. Assessment of the networks' ability to generalize

The ANNs developed so far were trained with 50% of data from all tubes. One can postulate that such networks only learn to "interpolate" between the *Re* numbers they were trained with and are unable to predict the performance of unknown geometries. The current section attempts to show that the 4-1 networks are indeed able to generalize.

Table 3 delineates the mean squared errors (MSE) of f_4LS_1LIN and j_4LS_1LIN networks trained with data from 2, 3, 4, 5, and 6 tubes and evaluated with all of the experimental data (8 tubes). Table 3 implies that the ANNs trained with selected tube data performed worse than the networks trained with 50% of data from all 8 tubes (see Table 2). However, if enough tubes were provided for training, the ANNs performed better than correlations (1) and (2). As expected, the network performance generally improved as additional tubes were put in the training basket. In the case of the f_4LS_1LIN network, 6 training tubes were needed to obtain satisfactory performance. The j_4LS_1LIN network was more perceptive and showed outstanding results with 4 training tubes. The networks' performance was sensitive to the randomly-generated initial guess, so the training procedure was repeated 10–20 times for each case, and only the best results were considered. The results summarized in Table 3 indicate that the 4LS-1LIN networks recommended in the previous section are able to generalize and correctly predict the performance of unknown geometries. Additional details about the networks summarized in Table 3 are given in Zdaniuk [3].

Table 3
MSE's of networks trained with selected tube data

Training tubes	MSE	
	f_4LS_1LIN	j_4LS_1LIN
1 and 5	1.321×10^{-5}	3.329×10^{-7}
1, 3, and 5	9.290×10^{-7}	2.324×10^{-7}
1, 3, 5, and 7	6.438×10^{-7}	8.794×10^{-9}
1, 3, 4, 5, and 7	7.060×10^{-7}	1.668×10^{-8}
1, 3, 4, 5, 7, and 8	4.713×10^{-8}	6.442×10^{-9}

5. Evaluation of *f*- and *j*-networks with independent experimental data

In this section, independent experimental data are used to evaluate the performance of two f_4LS_1LIN and j_4LS_1LIN networks. Because of their superior performance on the current data set, ANNs trained with 50% of experimental data from all tubes and ANNs trained with 6 out of 8 tubes were chosen for evaluation. Experimental results of Webb et al. [27] and Jensen and Vlakancic [28] were used as targets.

Table 4(a) provides the internal geometry of the tubes tested by Webb et al. [27]. Table 4(a) tubes are numbered W1 through W8 in order to distinguish them from the tubes used in the current study. Webb et al. [27] used a double-pipe counter-flow heat exchanger set up with liquid water on the inside and boiling R-12 on the annulus side. The water Reynolds number was varied between 20,000 and 80,000.

Jensen and Vlakancic [28] published experimental data for six helically-finned tubes outlined in Table 4(b). The tubes have been numbered JV1 through JV6 in order to distinguish them from the tubes tested in the current study. Jensen and Vlakancic [28] used two experimental test sections, one to obtain cooling results and one for heating results; however, only cooling results are considered here. Each test section was a double-pipe counter-flow water-to-water heat exchanger. The inside Reynolds number was varied between 10,000 and 72,000. Moreover, Jensen and Vlakancic [28] *Nu* numbers were converted into *j*-factor format (using a mean fluid and wall temperatures of 35 °C and 20 °C, respectively) in order allow direct evaluation of the *j* networks.

Table 5(a), Figs. 8 and 9 summarize the evaluation of the *f*- and *j*-networks with experimental data of Webb et al. [27]. The first conclusion drawn from the inspection

Table 4
Tubes tested by (a) Webb et al. [27], and (b) Jensen and Vlakancic [28]

Tube #	I.D. (mm)	e (mm)	p (mm)	t (mm)	N_s	α	e/D	p/e	p/D
(a) Tubes tested by Webb et al. [27]									
W1	15.54	Plain							
W2	15.54	0.327	1.08	0.265	45	45°	0.0210	2.81	0.0591
W3	15.54	0.398	1.63	0.28	30	45°	0.0256	3.50	0.0896
W4	15.54	0.43	4.88	0.325	10	45°	0.0277	9.88	0.273
W5	15.54	0.466	1.74	0.275	40	35°	0.0300	3.31	0.0993
W6	15.54	0.493	2.79	0.28	25	35°	0.0317	5.02	0.159
W7	15.54	0.532	4.19	0.28	25	25°	0.0342	7.05	0.241
W8	15.54	0.554	5.82	0.28	18	25°	0.0356	9.77	0.348
(b) Tubes reported by Jensen and Vlakancic [28]									
JV1	23.64	1.16	16.079	1.00	8	30°	0.0491	13.861	0.680
JV2	23.78	1.20	9.243	1.02	14	30°	0.0505	7.702	0.389
JV3	23.70	1.30	4.299	0.82	30	30°	0.0549	3.307	0.181
JV4	22.10	0.22	1.286	0.58	54	45°	0.00996	5.844	0.0582
JV5	24.13	0.33	1.404	0.90	54	45°	0.0137	4.254	0.0582
JV6	22.08	0.44	1.285	0.54	54	45°	0.0199	2.920	0.0582

Table 5
Evaluation of f- and j-networks with data of (a) Webb et al. [27], and (b) Jensen and Vlakancic [28]

f			j		
ANN:	MSE:	Performance shown on:	ANN:	MSE:	Performance shown on:
(a) Using data of Webb et al.[27]					
f_4LS_1LIN (trained w/ 50% of data from all tubes)	1.216×10^{-5}	Fig. 8	j_4LS_1LIN (trained w/ 50% of data from all tubes)	4.600×10^{-6}	Fig. 9
f_4LS_1LIN (trained w/ tubes 1, 3, 4, 5, 7, and 8)	2.756×10^{-5}		j_4LS_1LIN (trained w/ tubes 1, 3, 4, 5, 7, and 8)	4.198×10^{-6}	
(b) Using data of Jensen and Vlakancic [28]					
f_4LS_1LIN (trained w/ 50% of data from all tubes)	2.798×10^{-4}	Fig. 10	j_4LS_1LIN (trained w/ 50% of data from all tubes)	5.389×10^{-6}	Fig. 11
f_4LS_1LIN (trained w/ tubes 1, 3, 4, 5, 7, and 8)	1.995×10^{-5}		j_4LS_1LIN (trained w/ tubes 1, 3, 4, 5, 7, and 8)	4.709×10^{-6}	

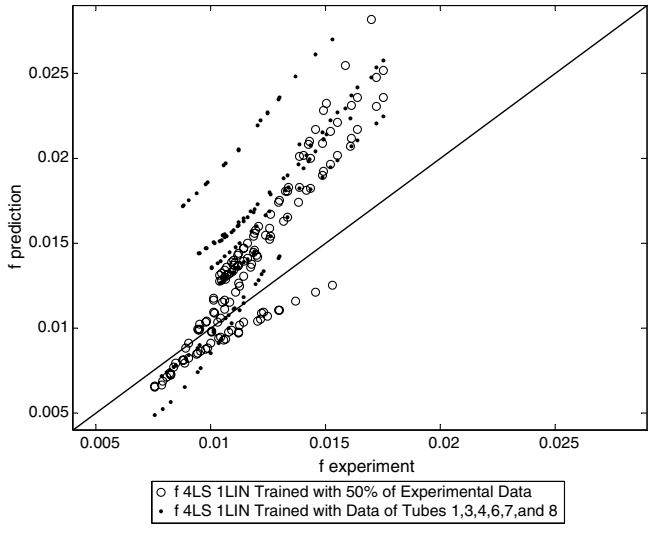

Fig. 8. Evaluation of f_4LS_1LIN networks with experimental data of Webb et al. [27].

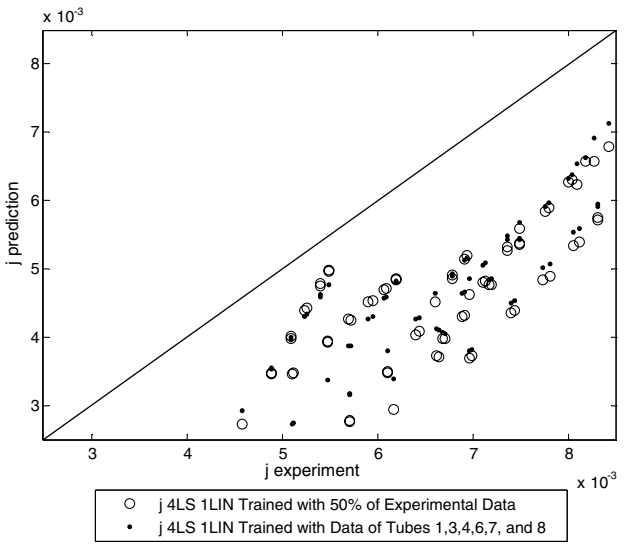

Fig. 9. Evaluation of j_4LS_1LIN networks with experimental data of Webb et al. [27].

of Figs. 8, 9 and Table 5(a) is that the neural networks do not predict the data of Webb et al. [27] very well. Webb et al.'s [27] friction data are over-predicted and heat transfer data under-predicted by the neural networks. The

results suggest a substantial difference in the experimental results between the current study and that of Webb et al. [27]. This conclusion is supported by the fact that there is no clear advantage of using networks trained with all of the tubes or with data from selected tubes, as indicated by Table 5(a).

Table 5(b), Figs. 10 and 11 summarize the evaluation of the *f*- and *j*-networks with experimental data of Jensen and Vlakancic [28]. Generally, the performance of the ANNs on the Jensen and Vlakancic [28] data was poor. The f_4LS_1LIN network trained with 50% of data from all tubes predicted negative friction factors for tube JV3 and over-predicted tube JV4's friction by as much as 400% (see Fig. 10). The networks trained with 6 out of 8 tubes performed slightly better than the ones trained with 50% of the entire data. Nevertheless, the errors associated with the *f*- and *j*-networks suggest that the data of Jensen and Vlakancic [28] demonstrate a different Reynolds number dependence than the data in the current study.

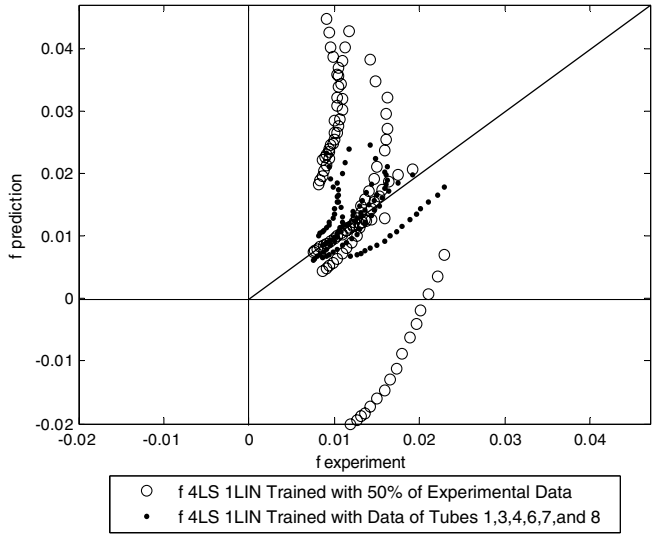

Fig. 10. Evaluation of f_4LS_1LIN networks with experimental data of Jensen and Vlakancic [28].

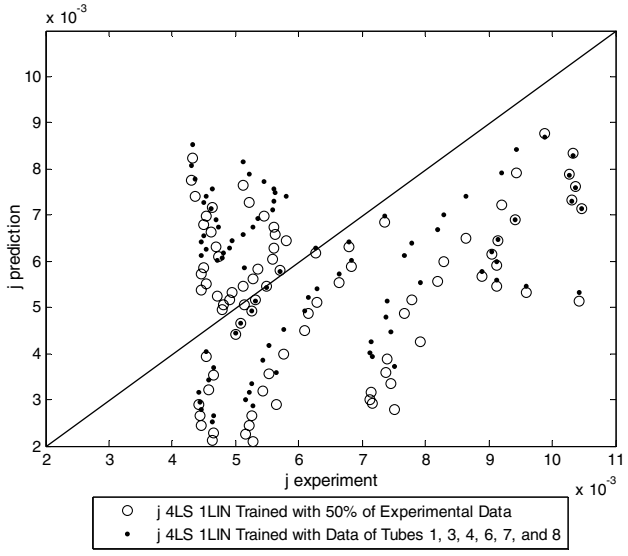

Fig. 11. Evaluation of j_4LS_1LIN networks with experimental data of Jensen and Vlakancic [28].

5.1. ANNs trained with a combined database

A common engineering practice is to average multiple measurements to obtain the "best" value. Therefore, a network trained with a database combining the results of Jensen and Vlakancic [28], Webb et al. [27], and the current study may prove to be a useful prediction tool. To create such a tool, an f_4LS_1LIN and a j_4LS_1LIN network were trained with 50% of data points (every other Reynolds number) from a database combining the experimental results of Webb et al. [27], Jensen and Vlakancic [28], and the current study. The performance of these two networks is depicted in Figs. 12 and 13, respectively. Both

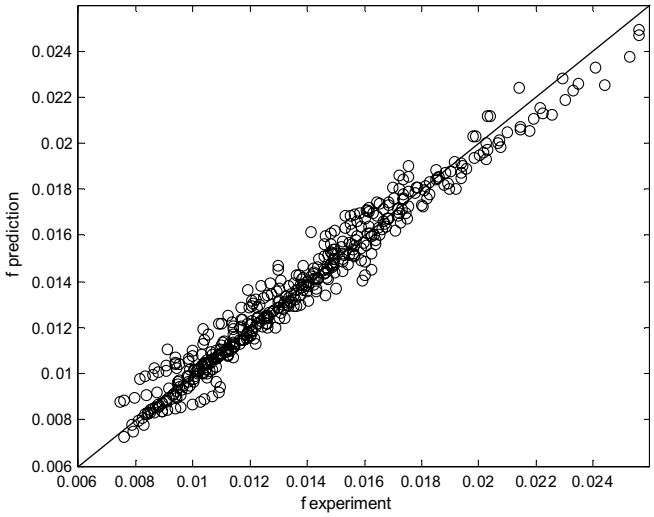

Fig. 12. Scatter plot showing the performance of the f_4LS_1LIN network trained with 50% of combined data.

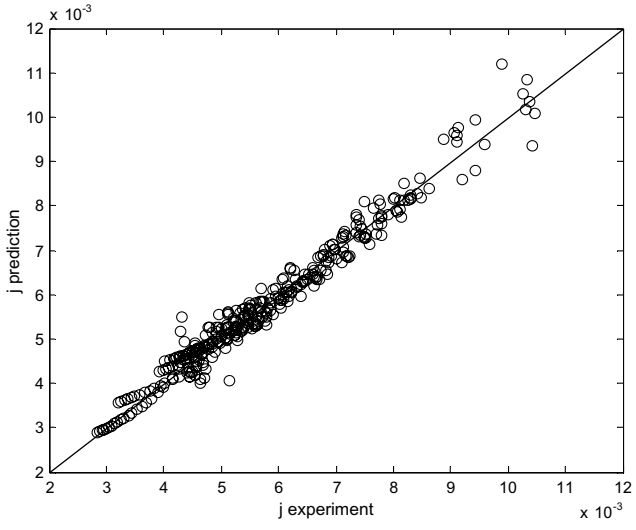

Fig. 13. Scatter plot showing the performance of the j_4LS_1LIN network trained with 50% of combined data.

figures show that the majority of data points from the combined set are predicted within 10% of the experiment. The mean squared errors (MSE) of the f_4LS_1LIN and j_4LS_1LIN networks are 4.553×10^{-7} and 7.671×10^{-8}, respectively, and are lower than the ones associated with Eqs. (1) and (2) applied to any of the data sets (cf. Zdaniuk et al. [23]). Based on the information presented so far, the f_4LS_1LIN and j_4LS_1LIN networks trained with 50% of data points from the combined database appear to be the best available prediction tool for friction and heat transfer in helically-finned tubes. The weights and biases for these two networks are:

- f_4LS_1LIN ANN trained with 50% of points from the combined database:

$$W^{1,0} = \begin{bmatrix} -7.2671 & -0.98217 & 2.0073 & 0.091471 \\ 7.5391 & 1.7808 & -2.2548 & -0.15899 \\ 3.5592 & -17.3752 & 4.0051 & -0.0099933 \\ -18.0686 & -9.384 & 4.6424 & 1.322 \end{bmatrix}$$

$$b^1 = \begin{bmatrix} 1.5625 \\ -1.8321 \\ 7.5575 \\ 12.0355 \end{bmatrix}$$

$$W^{2,1} = [13.8559 \;\; 13.3015 \;\; 0.77504 \;\; -0.70134] \quad b^2 = [-13.4947]$$

- j_4LS_1LIN ANN trained with 50% of points from the combined database:

$$W^{1,0} = \begin{bmatrix} -1.1545 & -0.068708 & -10.3588 & 2.0436 \\ -8.1534 & 62.9377 & -18.7554 & -0.12242 \\ 7.2905 & -127.338 & 16.7488 & 0.13477 \\ -108.2838 & -406.3062 & -595.2478 & 1.2132 \end{bmatrix}$$

$$b^1 = \begin{bmatrix} 2.5897 \\ -30.5346 \\ 68.2465 \\ \\ 402.9581 \end{bmatrix}$$

$$W^{2,1} = [-2.0141 \;\; -173.9585 \;\; -174.9652 \;\; 0.95102] \quad b^2 = [176.0276]$$

In order to gain total confidence that the neural network approach yields superior results, the ANNs trained with the combined database should be compared to algebraic correlations obtained with the combined database. A regression-based procedure used to correlate the experimental data of Webb et al. [27], Jensen and Vlakancic [28], and the current study yields the following equations for f and j:

$$f = 0.120 Re^{-0.260} N_s^{0.267} (e/D)^{0.385} \alpha^{0.276} \tag{10}$$

$$j = 0.0206 Re^{-0.219} N_s^{0.220} (e/D)^{0.468} \alpha^{0.544} \tag{11}$$

The performance of Eqs. (10) and (11) is depicted graphically in Figs. 14 and 15, respectively. The mean squared errors (MSE) are 5.343×10^{-6} for Eq. (10) and 1.071×10^{-6} for Eq. (11). Both errors are an order of magnitude higher than the MSEs associated with the neural network approach to correlate the combined database.

The current results show that ANNs perform extremely well on the data sets that they are trained with, but poorly on independent data, with experimental discrepancies being the most likely reason for disagreement. Most ANNs were capable of outperforming algebraic correlations, but the key aspect (other than the network's geometry and node functions) affecting the network performance was the selection of the training data set. This selection must be carried out carefully, so that there is enough variation in the inputs for the network to establish trends. The more data used in training process the better the network performance. However, using too many data points during the

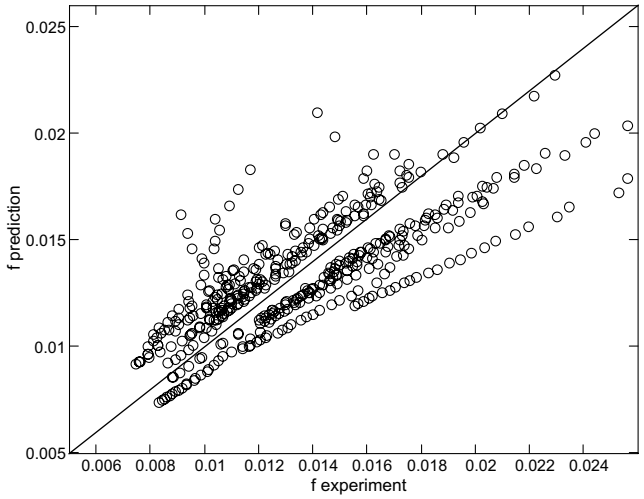

Fig. 14. Scatter plot showing the predictive performance of Eq. (10) for Fanning friction factor.

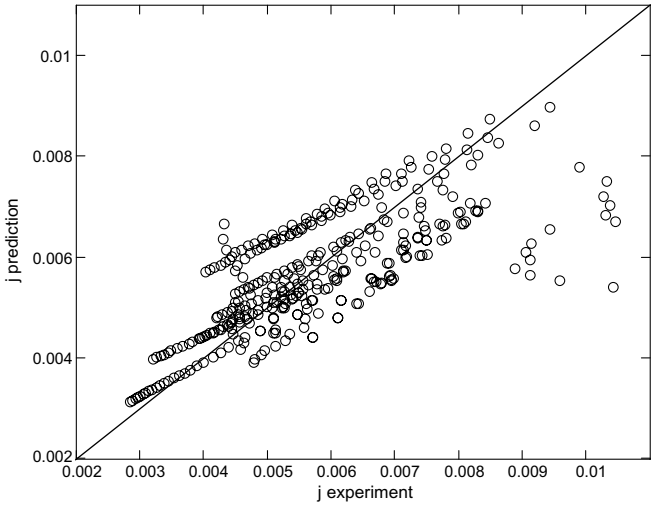

Fig. 15. Scatter plot showing the predictive performance of Eq. (11) for Colburn *j-factor*.

training process can negatively affect the network's ability to generalize.

6. Conclusions

The various network architectures tested in this work suggest the 4-1 feed-forward network with log-sigmoid node functions in the first layer and a linear node function in the output layer to be the most advantageous architecture to use for prediction of helically-finned tube performance. The 4LS_1LIN networks were accurate and were able to generalize, given adequate training data. Problems were encountered with data of other researchers, but these problems were almost certainly due to inherent differences in the experimental data, rather than to any fundamental shortcoming of the network itself. The three data sets contain possible bias errors, and ANNs learn to predict data without being capable of isolating measurement errors. Moreover, the power-law correlations (obtained with a least-squares regression that takes into account 100% of data points) also lacked appropriate accuracy (cf. Zdaniuk et al. [23]) when applied to the data of other researchers.

Considering the limited availability of heat transfer and friction data in helically-finned tubes, the recommended prediction tool for this type of tube is the f_4LS_1LIN and j_4LS_1LIN network trained with the combined results of Webb et al. [27], Jensen and Vlakancic [28], and the current study. The weights and biases for these two networks are given in this manuscript with additional details included in Zdaniuk [3].

The ultimate ANN would be trained with thousands of accurately measured data points from hundreds of different tubes and could predict friction factors and Colburn *j*-factors with virtually no error. Hence, neural network applications are well suited for manufacturers of heat exchange equipment, who can tap into their extensive databases to train state-of-the-art ANNs.

References

[1] R.L. Webb, Performance, cost effectiveness, and water-side fouling considerations of enhanced tube heat exchangers for boiling service with tube-side water flow, Heat Transfer Eng. 3 (1982) 84–98.

[2] G.J. Zdaniuk, L.M. Chamra, A literature review of friction and heat-transfer in helically-ribbed tubes, J. Enhanced Heat Transfer, submitted for publication.

[3] G.J. Zdaniuk, Heat Transfer and Friction in Helically-Finned Tubes using Artificial Neural Networks, Ph.D, dissertation, Mississippi State University, Mississippi State, MS, 2006.

[4] S. Haykin, Neural Networks: A Comprehensive Foundation, second ed., Prentice Hall, Upper Saddle River, NJ, 1999.

[5] K. Mehrotra, C.M. Mohan, S. Ranka, Elements of Artificial Neural Networks (Complex Adaptive Systems), The MIT Press, Cambridge, MA, 1996.

[6] J. Thibault, B.P.A. Grandjean, A neural network methodology for heat transfer data analysis, Int. J. Heat Mass Transfer 34 (8) (1991) 2063–2070.

[7] M. Sen, K.T. Yang, Applications of artificial neural networks and genetic algorithms in thermal engineering, in: F. Kreith (Ed.), The CRC Handbook of Thermal Engineering, CRC Press, Boca Raton, FL, 2000, pp. 620–661.

[8] S.A. Kalogirou, Applications of artificial neural networks in energy systems: a review, Energy Convers. Manage. 40 (1999) 1073–1087.

[9] S. Ashforth-Frost, V.N. Fontama, K. Jambunathan, S.L. Hartle, The role of neural networks in fluid mechanics and heat transfer, Proceedings of the 1995 IEEE Instrumentation and Measurement Technology Conference 1 (1995) 6–9.

[10] M.D. Kelleher, T.J. Cronley, K.T. Yang, M. Sen, Using artificial neural networks to develop a predictive method from complex experimental heat transfer data, Am. Soc. Mech. Eng. Heat Transfer Div. (HTD) 369 (5) (2001) 11–34.

[11] A. Pacheco-Vega, M. Sen, K.T. Yang, R.L. McClain, Prediction of humid air heat exchanger performance using artificial neural networks, Am. Soc. Mech. Eng. Heat Transfer Div. (HTD) 364 (3) (1999) 307–314.

[12] A. Pacheco-Vega, M. Sen, K.T. Yang, R.L. McClain, Heat rate predictions in humid air–water heat exchangers using correlations and neural networks, Trans. ASME: J. Heat Transfer 123 (3) (2001) 348–354.

[13] A. Pacheco-Vega, M. Sen, K.T. Yang, R.L. McClain, Neural network analysis of fin-tube refrigerating heat exchanger with limited experimental data, Int. J. Heat Mass Transfer 44 (2001) 763–770.

[14] G. Diaz, J. Yanes, M. Sen, K.T. Yang, R.L. McClain, Analysis of data from single-row heat exchanger experiments using an artificial neural network, Am. Soc. Mech. Eng. Fluids Eng. Div. (FED) 242 (1996) 45–52.

[15] G. Diaz, M. Sen, K.T. Yang, R.L. McClain, Simulation of heat exchanger performance by artificial neural networks, HVAC&R Res. 5 (3) (1999) 195–208.

[16] G. Diaz, M. Sen, K.T. Yang, R.L. McClain, On-line training of artificial neural networks for control of a heat exchanger test facility, Proc. National Heat Transfer Conf. 1 (2001) 359–365.

[17] G. Diaz, M. Sen, K.T. Yang, R.L. McClain, Dynamic prediction and control of heat exchangers using artificial neural networks, Int. J. Heat Mass Transfer 44 (2001) 1671–1679.

[18] Y. Islamoglu, A new approach for the prediction of the heat transfer rate of the wire-on-tube type heat exchanger – use of an artificial neural network model, Appl. Therm. Eng. 23 (2003) 243–249.

[19] A.J. Ghajar, L.M. Tam, S.C. Tam, Improved heat transfer correlation in the transition region for a circular tube with three inlet configurations using artificial neural networks, Heat Transfer Eng. 25 (2) (2004) 30–40.

[20] Y. Islamoglu, A. Kurt, Heat transfer analysis using ANNs with experimental data for air flowing in corrugated channels, Int. J. Heat Mass Transfer 47 (2004) 1361–1365.

[21] G. Scalabrin, L. Piazza, Analysis of forced convection heat transfer to supercritical carbon dioxide inside tubes using neural networks, Int. J. Heat Mass Transfer 46 (2003) 1139–1154.

[22] X.D. Chen, X.Y. Xu, S.K. Nguang, A.E. Bergles, Characterization of the effect of corrugation angles on hydrodynamic and heat transfer performance of four-start spiral tubes, Trans. ASME: J. Heat Transfer 123 (2001) 1149–1158.

[23] G.J. Zdaniuk, L.M. Chamra, P.J. Mago, Experimental determination of heat transfer and friction in helically-finned tubes, Exp. Therm. Fluid Sci., submitted for publication.

[24] M. Hagan, H. Demuth, M. Beale, Neural Network Design, PWS Publishing, Boston, MA, 1996.

[25] K. Levenberg, A method for the solution of certain problems in least squares, Quart. Appl. Math. 2 (1944) 164–168.

[26] D. Marquardt, An algorithm for least-squares estimation of nonlinear parameters, SIAM J. Appl. Math. 11 (1963) 431–441.

[27] R.L. Webb, R. Narayanamurthy, P. Thors, Heat transfer and friction characteristics of internal helical-rib roughness, Trans. ASME: J. Heat Transfer 122 (2000) 134–142.

[28] M.K. Jensen, A. Vlakancic, Experimental investigation of turbulent heat transfer and fluid flow in internally finned tubes, Int. J. Heat Mass Transfer 42 (1999) 1343–1351.